

## RESEARCH ARTICLE OPEN ACCESS

# Long-Term Application of No-Tillage-Induced Greater Risk of Poor Topsoil Aeration Along a European Pedoclimatic Gradient

Loraine ten Damme<sup>1</sup> | Marta Goberna<sup>2</sup> | Sara Sánchez-Moreno<sup>2</sup> | Mansonia Pulido-Moncada<sup>1</sup> | Laurent Philippot<sup>3</sup> | Mart Ros<sup>4</sup>  | Luca Bragazza<sup>5</sup>  | Sara Hallin<sup>6</sup> | Dalia Feiziene<sup>7</sup> | Lars Juhl Munkholm<sup>1</sup> 

<sup>1</sup>Department of Agroecology, Aarhus University, Foulum, Denmark | <sup>2</sup>Department of Environment and Agronomy, Instituto Nacional de Investigación y Tecnología Agraria y Alimentaria (INIA, CSIC), Madrid, Spain | <sup>3</sup>Université de Bourgogne, INRAE, Institut Agro, Dijon, France | <sup>4</sup>Wageningen Environmental Research, Wageningen University & Research, Wageningen, the Netherlands | <sup>5</sup>Agroscope, Field-Crop Systems and Plant Nutrition, Nyon, Switzerland | <sup>6</sup>Swedish University of Agricultural Sciences, Uppsala, Sweden | <sup>7</sup>Lithuanian Research Centre for Agriculture and Forestry, Institute of Agriculture, Akademija, Lithuania

**Correspondence:** Loraine ten Damme ([ltid@agro.au.dk](mailto:ltid@agro.au.dk))

**Received:** 25 October 2024 | **Revised:** 14 January 2025 | **Accepted:** 16 February 2025

**Funding:** This work was financially supported by the European Joint Programme for Soil (EJP SOIL) (Grant agreement No 862695) under the European Union's Horizon 2020 programme.

**Keywords:** gas diffusivity | long-term agricultural field experiments | soil gas transport | soil structure | tillage

## ABSTRACT

This paper assesses the effect of long-term contrasting tillage practices on topsoil structural characteristics critical for nitrous oxide (N<sub>2</sub>O) emissions and carbon sequestration across a pedoclimatic gradient. The hypotheses tested are that: (i) aeration is greater in the topsoil of ploughed (to 0.20–0.30 m depth) than in no-till soils and (ii) the effect of tillage practice on soil functionality depends on the context, and thus varies between sites with different pedoclimatic conditions. We evaluated the topsoil characteristics of seven long-term tillage experiments, spread along a 2600-km transect in Europe. A total of 576 soil cores (100-cm<sup>3</sup>) were sampled from 0 to 0.10 and 0.10 to 0.20 m depths in mouldboard-ploughed and no-tillage treatments after harvest. The soil water content at –30, –60, and –100 hPa matric potential was measured as well as air permeability ( $k_a$ ) and relative gas diffusivity ( $D_s/D_o$ ) at –100 hPa, from which soil bulk and gas transport characteristics were derived. Despite large variations in the characteristics among sites, tillage did significantly affect the characteristics across sites. The degree of compactness was less and total pore volume was greater in the ploughed than in the no-till treatments. Still, thresholds indicating suitable conditions for root growth were largely met under both practices. The ploughed soils showed vertical stratification, with a better aeration of the 0–0.10 m soil layer compared to the 0.10–0.20 m layer. No differences were observed between the ploughed 0.10–0.20 m and no-till layers, which were attributed to soil settlement after ploughing. While the  $D_s/D_o$  at 0.10–0.20 m depth was favourable for promoting N<sub>2</sub>O emissions, the water-filled pore space was below suggested thresholds. Impacts of tillage on soil structural and functional characteristics were both significant and generalisable but also deviated locally. For example,  $D_s/D_o$  and  $k_a$  generally increased with the air-filled pore volume ( $\epsilon_a$ ), yet sites with greater  $\epsilon_a$  did not necessarily have higher  $D_s/D_o$  and  $k_a$ . Existing models explaining  $D_s/D_o$  and  $k_a$  with  $\epsilon_a$  were fitted to the measured data and performed best when both depths and tillage practices were assessed altogether. Despite the limited differences at –100 hPa, anoxic conditions may in reality prevail for a longer period under no-till than ploughing.

This is an open access article under the terms of the [Creative Commons Attribution-NonCommercial-NoDerivs](https://creativecommons.org/licenses/by-nc-nd/4.0/) License, which permits use and distribution in any medium, provided the original work is properly cited, the use is non-commercial and no modifications or adaptations are made.

© 2025 The Author(s). *European Journal of Soil Science* published by John Wiley & Sons Ltd on behalf of British Society of Soil Science.

## Summary

- Effect of ploughing and no-till on topsoil structure characterised across 7 European long-term field experiments
- Differences among sites were larger than between tillage practices or soil depths at a given site
- Still, the impacts of ploughing or no-tillage on soil structure were significant and generalisable.
- The ploughed 0–0.10 m layer was most aerated and with the smallest risk of anoxic soil processes.

## 1 | Introduction

The drive for a more sustainable management of agricultural soils requires an improved understanding of the impact of tillage strategies on soil structure, specifically in relation to trade-offs and synergies with carbon (C) sequestration and nitrous oxide (N<sub>2</sub>O) emissions. Conservation tillage avoids adverse effects of ploughing, such as the disruption of biopores and fungal and microbial networks (Lucas et al. 2019; Or et al. 2021) while improving a number of soil properties, such as aggregate stability, pore connectivity, and hydraulic conductivity (Blanco-Canqui and Ruis 2018; Hill 1990; Vogeler et al. 2009). However, concerns have been raised about elevated N<sub>2</sub>O emissions and nutrient losses under reduced tillage (Maenhout et al. 2024; O'Neill et al. 2020; Six et al. 2004; van Kessel et al. 2013; Wardak et al. 2022) due to increased soil compactness, greater accumulation of organic matter in the upper soil layers, and an increased diversity and abundance of fungal denitrifiers (Bösch et al. 2022; Gómez-Muñoz et al. 2021; Meurer et al. 2018; van Ouwerkerk and Boone 1970).

Global meta-analyses indicate that the effect of tillage practices on greenhouse gas fluxes varies with climate, soil texture, time since implementation, and soil management (e.g., Huang et al. 2018; Maenhout et al. 2024; Rochette 2008; Shalokor et al. 2021; van Kessel et al. 2013). Maenhout et al. (2024) concluded, however, that existing research provides insufficient evidence to draw general conclusions on the effect of tillage practices on synergies and trade-offs between the C and nitrogen (N) cycles. The authors highlighted, for example, the lack of information about the impact of pedoclimatic constraints and the need for the evaluation of long-term practices. Mondal and Chakraborty (2022) performed a meta-analysis on the effect of tillage practices on soil aggregation and the pore size distribution, showing that coarse-textured soils are susceptible to decreasing macroporosity under no-till practices, but long-term adaptation can alleviate the impact. The impact of long-term tillage practices on soil functionality specifically has been assessed locally and indicated greater topsoil porosity and gas conductivity under ploughed than under no-till practices (e.g., Abdollahi and Munkholm 2017; Cooper et al. 2021; Martínez et al. 2016; Petersen et al. 2008; Schlüter et al. 2018; Talukder et al. 2022). However, a comprehensive assessment across a pedoclimatic gradient is still lacking.

Understanding the impact of tillage on soil structure is essential. For instance, soil structure drives root growth—and thus plays an important role in C sequestration (Colombi et al. 2019; Kätterer et al. 2011; Lucas et al. 2023), through facilitation and restriction of penetration, soil-root contact, and aeration. The soil's aeration status also determines the end-product of decomposition of soil organic matter, with carbon dioxide (CO<sub>2</sub>) and methane (CH<sub>4</sub>) being produced under oxic and anoxic conditions, respectively. Nitrous oxide is produced under both oxic and anoxic soil conditions as a by-product of nitrification and an intermediate of denitrification, respectively (Butterbach-Bahl et al. 2013; Hallin et al. 2018). Even so, in temperate climates most soil N<sub>2</sub>O emissions result from denitrification and are driven by a high soil water content (Bateman and Baggs 2005; Elberling et al. 2023; O'Neill et al. 2020), rewetting of dry soil (Harris et al. 2021), and freeze–thaw cycles (Wagner-Riddle et al. 2017), provided sufficiently degradable C and N (Bösch et al. 2022).

Several indicator thresholds have been suggested for characterising (an)oxic soil conditions. Ample air space, for example, 10%–15% (Grable and Siemer 1968; Wesseling and van Wijk 1957) or roughly 10% of pores larger than 30 µm (Dexter 1988), is not necessarily sufficient to support oxic soil processes because these bulk soil properties do not reflect conditions at microscale, among which is the position of hotspots created by particulate organic matter (Lucas et al. 2024). Moreover, the transport of gases through soil requires advection and diffusion. Advection and diffusion are both affected by soil pore connectivity, continuity, and tortuosity of the soil structure, but in different ways (Arthur et al. 2012; Ball et al. 1988; Martínez et al. 2016). Advection, expressed in terms of air permeability ( $k_a$ ), is controlled by the larger pore diameters, whereas diffusion, expressed in terms of relative gas diffusivity ( $D_s/D_o$ ), is largely controlled by the air-filled pore volume ( $\epsilon_a$ ) and is, in principle, independent of pore size (Kuncoro et al. 2014; Moldrup et al. 2000). Soil water indicators such as the water-filled pore space (WFPS) are also used, particularly in relation to denitrification and respiration (e.g., Badagliacca et al. 2018; Cosentino et al. 2013; Fernández-Ortega et al. 2023; O'Neill et al. 2020), but WFPS may not express changes in soil aeration accurately (Balaine et al. 2016; Pulido-Moncada et al. 2022).

The main aim of this study is to evaluate the impact of long-term (>12 years), contrasting tillage practices on soil structural characteristics of the upper soil layer (0–0.20 m depth) using seven long-term field experiments from across Europe, covering sites with differences in pedoclimatic conditions. The objectives of this study were to: (1) Assess the overall impact of tillage practices and geographic location on soil bulk and gas transport characteristics of the topsoil across a pedoclimatic gradient; (2) Assess the performance of established models of soil gas transport characteristics across locations, tillage practices, and soil depths; and (3) Evaluate the consequences for soil functioning specifically considering the risks for N<sub>2</sub>O emissions. The hypotheses of this study are that: (i) aeration is greater in the topsoil of ploughed soils than in no-till soils, and (ii) the effect of tillage practice on soil functionality depends on the context, and thus varies between sites with different pedoclimatic conditions.

## 2 | Materials and Methods

A range of soil structural characteristics was assessed for different tillage practices in seven long-term agricultural field experiments spread along a pedoclimatic gradient in Europe (Section 2.1). The measurements (Section 2.2) were done in the laboratory at Aarhus University, Viborg (Denmark) on minimally disturbed soil samples. The sampling campaign took place after harvest, prior to any consecutive field operations, in the second half of 2021.

### 2.1 | Experimental Sites and Treatments

The seven long-term tillage experiments considered in this study were spread along a pedoclimatic gradient across Europe (Figure S1), with sites in Sweden (SE, Camobisol), Lithuania (LT, Cambisol), Denmark (DK, Umbrisol), the Netherlands (NL, Cambisol), Switzerland (CH, Cambisol), France (FR, Luvisol) and Spain (ES, Cambisol). At the time of sampling, the tillage experiments had been running for 12–51 years (Table 1). Each experimental site (hereafter referred to as location) included four blocks, in which the following experimental treatments were practised: annual mouldboard ploughing to 0.20–0.30 m depth, reduced-till, and no-till with direct seeding. In this study, the two contrasting treatments, no-till and ploughed, were considered, while the reduced-till was excluded because of the varying tillage intensity (ranging from superficial tillage to chisel ploughing to 0.20 m depth (Sánchez-Moreno et al. 2024)). The Dutch no-till treatment was cultivated with vibrating tines to 0.012–0.015 m depth as part of seedbed preparation. The measured data of the reduced-till treatment is available online (ten Damme et al. 2024).

The crop prior to soil sampling in 2021 was grain maize (*Zea mays*) at the Swiss site (Trial P\_29C), winter barley (*Hordeum vulgare*) at the Dutch site (BASIS-CONV), and winter wheat (*Triticum aestivum*) at the remaining locations. Further details on the crop rotation can be found in the Supporting Material of this study and in Sánchez-Moreno et al. (2024). The ploughed treatment of the Swiss site was last ploughed in April 2021 and those at the other sites in autumn 2020. Cover crops are part of the rotations at the French site (Boigneville), the Danish site (CENTS Foulum) when no winter crop is sown, and usually at the Dutch site but not in the year prior to sampling. Crop residues were retained at all sites. The sites were rain-fed and subjected to chemical weed control. The sampled plots at the Dutch site were not fertilised, whereas the others received mineral NPK-fertiliser at varying rates.

The sites' basic soil characterisation in terms of the particle size distribution, soil organic matter (SOM) content, and dry bulk density ( $\rho_b$ ) are reported in Table 2. The particle size distribution and soil organic matter content were derived from disturbed composite soil samples (five subsamples per block, treatment, and soil depth) following the sampling protocol by Fernández-Ugalde et al. (2018). The particle size distribution (ten Damme et al. 2024) was determined using the pipette method (Gee and Bauder 2018). The soil organic matter content was assumed to be a factor of 2 of total organic carbon, i.e., assuming that organic matter exists for 50% of carbon

(Pribyl 2010), with the total organic carbon (ten Damme et al. 2024) measured by an Elemental LECO TruSpec CN element analyser (Leco Corp. MI, USA) in air-dried ground soil samples after a 55°C acidic (HCl) treatment. The dry bulk density was calculated after oven-drying the minimally disturbed soil samples (Section 2.2.2).

### 2.2 | Soil Structural Characterisation

#### 2.2.1 | Soil Sampling

At each location, 10 minimally disturbed soil samples (100 cm<sup>3</sup> steel cylinders, 34 mm high and 60 mm inner diameter) were taken in each block and treatment: five from 0 to 0.10 m depth and five from 0.10 to 0.20 m depth. Each set of five samples was taken in a specific distribution, with a centre sample and four samples taken at 1–2 m distance (depending on plot size), at 90° intervals, around the centre sample, that is, following the LUCAS sampling protocol of Fernández-Ugalde et al. (2018). However, at the Danish site, the wheel tracks interfered with this sampling design, and instead, samples were taken at two ends of each plot. The Danish team sampled three samples along a transect of approximately 1 m in each end, totalling six per depth per plot, to comply with other projects using the site.

The soil samples were stored at 2°C–4°C until transported to laboratory facilities at Aarhus University Viborg, Denmark. The soil samples were weighed for estimation of the soil water content at the time of sampling before they were used in soil structural characterisation as described below. The soil water status at the time of sampling was close to –100 hPa matric potential at the Dutch, Danish, and Lithuanian (Kédainiai) sites and more negative for the remaining countries, with relatively dry conditions at the Spanish (INIA-LTE-ROT) site (Figure S2).

#### 2.2.2 | Laboratory Measurements

The soil cores were saturated on tension tables, then successively drained to –30, –60, and –100 hPa matric potential. At each matric potential, the samples were weighed. At –100 hPa matric potential, air permeability and gas diffusivity were measured. Air permeability was measured in an apparatus designed and described by Schjønning and Koppelgaard (2017). In short, the volumetric airflow rate through the soil sample is recorded at pressure differences of 5, 2, 1, and 0.5 hPa. The airflow at 5 hPa yields the apparent air permeability ( $k_{a-5\text{hPa}}$ ,  $\mu\text{m}^2$ ), while the airflow at an infinitesimal pressure gradient, based on the Forchheimer polynomial regression of the measured flow-pressure data, yields the true or Darcian air permeability ( $k_a$ ,  $\mu\text{m}^2$ ). Soils are typically classified as 'impermeable' at  $1 \mu\text{m}^2 k_a$  (Ball et al. 1988) or 'slowly permeable' up to  $20 \mu\text{m}^2 k_a$  (Fish and Koppi 1994). Gas diffusivity was measured using the one-chamber, one-gas method as described by Schjønning et al. (2013a). The measurements allow calculations of the relative gas diffusivity ( $D_s/D_o$ , –) by relating the gas diffusion coefficient in the soil ( $D_s$ ,  $\text{cm}^2 \text{s}^{-1}$ ) to the diffusion of O<sub>2</sub> in air ( $D_o$ :  $0.205 \text{cm}^2 \text{s}^{-1}$ ). Critically low values of  $D_s/D_o$  for supporting aerobic microbial activity range from 0.005 to 0.020, with coarser soils requiring higher rates (Schjønning et al. 2003; Stepniewski 1981). Afterwards, the soil samples were

**TABLE 1** | Specification of the tillage-experiments. The numbers in the first column refer to the locations shown in Figure S1. Crop rotation is provided in Data S1. Table is adapted from the metadata at <https://doi.org/10.5281/zenodo.12515043> (Sánchez-Moreno et al. 2024).

Location	Site	Experiment	Starting year	Geographic coordinates	Climate (Köppen classification)	Average yearly rainfall (mm)	Average temperature of the coldest/warmest month (°C)			Soil taxonomy <sup>a</sup>	Soil texture <sup>b</sup>	Crop <sup>c</sup>
1	DK	CENTS Foulum	2002	56.50, 9.583	Temperate oceanic climate (Cfb)	558	1.20/16.45		Luvic Umbrisol	Sandy loam	Winter wheat	
2	LT	Kėdainiai	1999	55.390, 23.872	Warm-summer humid continental (Dfb)	695	−4.6/17.8		Cambisol	Sandy loam	Winter wheat	
3	NL	BASIS-CONV	2009	52.544, 5.576	Atlantic Central	833	2.0/16.6		Cambisol	Loam	Spring barley	
4	ES	INIA-LTE-ROT	1994	40.516, −3.310	Cold semi-arid climate (Bsk)	315.5	5.1/26.3		Cambisol	Loam	Winter wheat	
5	CH	Trial P_29C	2007 <sup>d</sup>	46.398, 6.24	Temperate oceanic climate (Cfb)	940	2.2/21		Cambisol	Silty loam	Grain maize	
6	SE	Lanna/R2-4010	1974	58.346, 13.120	Transition between Temperate oceanic (Cfb) and Warm-summer humid continental (Dfb)	558	−1.8/18.2		Cambisol	Silty clay	Winter wheat	
7	FR	Boigneville	1970	48.335, 2.374	Oceanic climate (Cfb)	615.16	4.3/19.9		Neoluvisol	Silty loam	Winter wheat	

Abbreviations: CH, Switzerland; DK, Denmark; ES, Spain; FR, France; LT, Lithuania; NL, the Netherlands; SE, Sweden.

<sup>a</sup>WRB (2022).

<sup>b</sup>Particle size distribution given in Table 2.

<sup>c</sup>Crop grown in the season prior to soil sampling.

<sup>d</sup>Field experiment established in 1969, with no-till treatments included since 2007.

**TABLE 2** | Basic soil characteristics of the sites, per depth and tillage treatment (arithmetic mean values  $\pm$  standard deviation,  $n = 4$ ).

Soil depth (m)	Site	Particle size distribution			Ploughed		No-till	
		Clay ( $< 2 \mu\text{m}$ )	Silt (2–50 $\mu\text{m}$ )	Sand (50– 2000 $\mu\text{m}$ )	Soil organic matter (SOM)	Dry bulk density ( $\rho_b$ )	Soil organic matter (SOM)	Dry bulk density ( $\rho_b$ )
		g 100 g <sup>-1</sup>			g 100 g <sup>-1</sup>	Mg m <sup>-3</sup>	g 100 g <sup>-1</sup>	Mg m <sup>-3</sup>
0–0.10	DK	6 $\pm$ 1.5	26 $\pm$ 3.7	68 $\pm$ 2.8	4.9 $\pm$ 1.1	1.20 $\pm$ 0.08	5.2 $\pm$ 0.6	1.26 $\pm$ 0.12
	LT	13 $\pm$ 2.7	34 $\pm$ 3.2	53 $\pm$ 1.3	2.6 $\pm$ 0.2	1.50 $\pm$ 0.08	2.6 $\pm$ 0.2	1.55 $\pm$ 0.04
	NL	18 $\pm$ 1.4	32 $\pm$ 1.8	50 $\pm$ 2.6	2.4 $\pm$ 0.2	1.39 $\pm$ 0.07	3.5 $\pm$ 1.3	1.41 $\pm$ 0.05
	ES	22 $\pm$ 3.8	38 $\pm$ 2.5	40 $\pm$ 4.6	1.5 $\pm$ 0.1	1.42 $\pm$ 0.16	2.1 $\pm$ 0.3	1.45 $\pm$ 0.11
	CH	22 $\pm$ 4.0	52 $\pm$ 2.6	26 $\pm$ 2.1	3.4 $\pm$ 0.7	1.37 $\pm$ 0.10	4.2 $\pm$ 0.4	1.30 $\pm$ 0.08
	SE	43 $\pm$ 4.4	47 $\pm$ 3.4	10 $\pm$ 1.2	2.2 $\pm$ 0.7	1.15 $\pm$ 0.06	6.3 $\pm$ 1.2	1.08 $\pm$ 0.07
	FR	23 $\pm$ 1.9	69 $\pm$ 1.4	8 $\pm$ 1.0	3.4 $\pm$ 0.2	1.08 $\pm$ 0.18	4.7 $\pm$ 0.4	1.18 $\pm$ 0.11
0.10–0.20	DK	6 $\pm$ 1.3	26 $\pm$ 2.8	68 $\pm$ 2.5	4.7 $\pm$ 0.9	1.25 $\pm$ 0.08	4.3 $\pm$ 0.7	1.36 $\pm$ 0.08
	LT	12 $\pm$ 2.0	33 $\pm$ 1.9	54 $\pm$ 1.8	2.4 $\pm$ 0.2	1.61 $\pm$ 0.11	1.9 $\pm$ 0.9	1.63 $\pm$ 0.04
	NL	19 $\pm$ 1.0	32 $\pm$ 2.0	49 $\pm$ 2.7	2.3 $\pm$ 0.3	1.47 $\pm$ 0.07	2.3 $\pm$ 0.2	1.47 $\pm$ 0.10
	ES	23 $\pm$ 3.5	38 $\pm$ 2.1	39 $\pm$ 3.9	1.4 $\pm$ 0.2	1.42 $\pm$ 0.11	1.4 $\pm$ 0.1	1.44 $\pm$ 0.10
	CH	22 $\pm$ 3.2	52 $\pm$ 1.8	27 $\pm$ 1.6	3.3 $\pm$ 0.4	1.39 $\pm$ 0.07	3.1 $\pm$ 0.2	1.40 $\pm$ 0.12
	SE	45 $\pm$ 3.3	45 $\pm$ 3.0	9 $\pm$ 0.9	5.9 $\pm$ 0.6	1.34 $\pm$ 0.05	6.2 $\pm$ 1.3	1.38 $\pm$ 0.07
	FR	24 $\pm$ 1.1	68 $\pm$ 1.2	8 $\pm$ 1.4	2.6 $\pm$ 0.1	1.30 $\pm$ 0.15	2.9 $\pm$ 0.1	1.31 $\pm$ 0.10

oven-dried at 105°C to obtain the dry mass, hence dry bulk density ( $\rho_b$ , Mg m<sup>-3</sup>).

### 2.2.3 | Calculations

Soil density is expressed as the degree of compactness ( $DC$ , %, Equation 1), that is, as the dry bulk density as a percentage of a reference density ( $\rho_{\text{ref}}$ , Mg m<sup>-3</sup>, Håkansson 1990). The  $\rho_{\text{ref}}$  was calculated from the soil particle distribution and soil organic matter content as suggested by (Keller and Håkansson 2010, equation 12). The total pore volume ( $\theta$ , m<sup>3</sup> m<sup>-3</sup>), volumetric soil water content ( $\theta_v$ , m<sup>3</sup> m<sup>-3</sup>), air-filled pore volume ( $\epsilon_a$ , m<sup>3</sup> m<sup>-3</sup>) and water-filled pore space ( $WFPS$ , %, Equation 2) were calculated for each sample at each matric potential (i.e., at -30, -60 and -100 hPa). These calculations are based on estimates of the soil particle density ( $\rho_p$ , Mg m<sup>-3</sup>) for the combination of block, treatment, and soil depth per site. The  $\rho_p$  was estimated using pedotransfer functions established by (Schjønning et al. 2017, equations 10 and 11), that is, based on the clay and soil organic matter contents.

$$DC = 100 \frac{\rho_b}{\rho_{\text{ref}}} \quad (1)$$

$$WFPS = \left[ \frac{\theta_v}{\theta} \right] * 100 \quad (2)$$

The  $\epsilon_a$  at known matric potentials reflects the pore volume of pores with certain diameters, following the Young-Laplace (Young 1805) equation. Consequently,  $\epsilon_a$  at -30, -60, and -100 hPa is made up of pores with a diameter  $\geq 100 \mu\text{m}$

( $\epsilon_{a-\theta \geq 100 \mu\text{m}}$ ),  $\geq 50 \mu\text{m}$  ( $\epsilon_{a-\theta \geq 50 \mu\text{m}}$ ) and  $\geq 30 \mu\text{m}$  ( $\epsilon_{a-\theta \geq 30 \mu\text{m}}$ ), respectively. Soil gas transport characteristics were calculated for the soil cores equilibrated to -100 hPa matric potential. These characteristics encompassed the ratio  $R$  (-), specific diffusivity ( $SD$ , -), and the average effective pore diameter ( $d_{\text{eff}}$ ,  $\mu\text{m}$ ) (Equations 3–5). The ratio  $R$  assesses whether the effective air permeability follows laminar flow conditions or turbulent air flow (Schjønning and Koppelgaard 2017), with higher ratios indicating more turbulent air flow (Schjønning 2019). The specific diffusivity has been introduced as a measure of pore tortuosity (Gradwell 1961), with lower values indicating increased tortuosity, decreased connectivity, or a combination of both (Schjønning et al. 2013b). While there are different parameters to assess pore tortuosity (e.g., Ball et al. 1988), specific diffusivity is considered an unbiased evaluation due to its empirical relation of directly measured variables. The average effective pore diameter directly relates to gas transport characteristics and reflects the average effective diameter of a tortuous tube system (Ball 1981a).

$$\text{ratio } R = \frac{k_{a-5hPa}}{k_a} \quad (3)$$

$$SD = \frac{D_s/D_o}{\epsilon_a} \quad (4)$$

$$d_{\text{eff}} = 2 \sqrt{\frac{8 k_a}{D_s/D_o}} \quad (5)$$

The relationship between  $D_s/D_o$  and  $\epsilon_{a-100}$  was evaluated using three models: the model suggested by Buckingham (1904) in

which  $D_s/D_0$  simply follows a power function of  $\varepsilon_a$  (Equation 6), the water-induced linear reduction (WLR) model as described by Marshall (1959) (Equation 7) where  $\varnothing$  is the total pore volume, and the macroporosity-dependent (MPD) model suggested by Moldrup et al. (2000) (Equation 8), where  $a$ ,  $b$ , and  $c$  are coefficients.

$$D_s/D_0 = \varepsilon_a^b \tag{6}$$

$$D_s/D_0 = \frac{\varepsilon_a^b}{\varnothing} \tag{7}$$

$$D_s/D_0 = a \cdot \varepsilon_a^b + c \cdot \varepsilon_a \tag{8}$$

The relationships between  $k_a$  and  $\varepsilon_a$  were evaluated following the approach by Ball et al. (1988), that is, based on log–log scales.

### 2.2.4 | Statistical Analyses

The primary objective was to test for differences in terms of tillage practice (ploughed and no-till), soil depth (0–0.10 and 0.10–0.20 m) and their interaction. The location was added as a main effect primarily to investigate if an effect of tillage, depth, or their interaction differed between locations, but also to investigate spatial differences. Block was added as a random effect to account for potential between-block variation. Thirty-one samples out of 576 were excluded from the analyses based on the observations in the lab that these cylinders did not have the same sample volume as the other cores. For these samples, dry bulk density and  $\varepsilon_a$  and derivatives could not be accurately calculated. With the remaining 576 samples, block averages were calculated per site, tillage practice, and soil depth prior to statistical analyses.

The soil structural characteristics were fitted using the linear mixed-effects model (lmer) from the R-package lme4 version 1.1–35.4 (Bates et al. 2015), response~Treatment×Depth×Site+(1|Block). A contrast specification (sum-to-zero for tillage practice, soil depth and site) was provided using the ‘contr.sum’ function for acquiring the type 3 sums of squares. A log10 transformation was applied to  $k_a$ , for which the response values were provided as geometric means. The assumptions in terms of normal distribution of the residuals and heteroscedasticity were checked visually. We used the type III ANOVA to compute analyses of variance tables and performed the posthoc test emmeans from the R-package emmeans version 1.10.2 (Lenth 2024) for the main factors when  $p < 0.05$ .

ANOVA was also employed to compare models describing  $D_s/D_0$  and  $k_a$  with  $\varepsilon_a$  for the different tillage treatments and soil depths. The goodness of fit of the models was assessed using the AIC (Akaike information criterion) command in R. The performances were further evaluated based on  $R^2$  and RMSE.

## 3 | Results

### 3.1 | Ranges of Topsoil Bulk Properties and Gas Transport Characteristics for the Different Sites

The estimated mean values of the soil bulk properties and pore conductivity characteristics varied significantly among locations (Table 3, see also Figure S3). For example, the highest

**TABLE 3** | Analysis of variance of the soil bulk and soil pore conductivity characteristics. Significant differences in plain font (i.e., not underlined and bold) are overruled by an interaction effect.

Experimental factors	DC	$\varnothing$	$\varepsilon_{a-30}$	$\varepsilon_{a-60}$	$\varepsilon_{a-100}$	WFPS <sub>-30</sub>	WFPS <sub>-60</sub>	WFPS <sub>-100</sub>	$D_s/D_0$	SD <sup>a</sup>	$k_a$	Ratio R <sup>a</sup>	$d_{eff}^a$
Tillage treatment×Soil depth×Location	ns	ns	ns	ns	ns	ns	ns	ns	ns	ns	ns	ns	*
Tillage treatment×Soil depth	ns	ns	**	**	*	***	**	**	*	ns	ns	ns	ns
Tillage treatment×Location	ns	ns	ns	ns	ns	ns	ns	ns	*	ns	***	***	*
Soil depth×Location	***	***	***	***	***	***	***	***	***	ns	***	**	ns
Tillage treatment	**	**	**	**	***	*	**	**	*	ns	ns	ns	ns
Soil depth	***	***	***	***	***	***	***	***	***	***	***	ns	ns
Location	***	***	***	***	***	***	***	***	***	***	***	***	***

Note:  $\varepsilon_a$ , air-filled pore volume at −30, −60, and −100 hPa matric potential;  $\varnothing$ , total pore volume;  $d_{eff}$ , average effective pore diameter;  $D_s/D_0$ , relative gas diffusivity;  $k_a$ , Darcian air permeability; ns =  $p > 0.05$ .

Abbreviations: DC, degree of compactness; Ratio R, ratio of air permeability; SD, specific gas diffusivity; WFPS, water-filled pore space at −30, −60, and −100 hPa matric potential.

<sup>a</sup> At −100 hPa matric potential.

\*\*\* $p < 0.001$ .

\*\* $p < 0.01$ .

\* $p < 0.05$ .

degree of compactness ( $DC$ ) was observed at the Lithuanian site (97%), whereas the other sites were characterised by a degree of compactness of between 89% (Swedish site) and 85% (Spanish site). The air-filled pore volume ( $\epsilon_a$ ) at  $-100$  hPa matric potential ranged from  $0.14$  to  $0.23 \text{ m}^3 \text{ m}^{-3}$  across sites. The  $WFPS$  at  $-100$  hPa matric potential ( $WFPS_{-100}$ ) ranged from 56% to 70% across sites, with the Danish site having the lowest value and the Dutch site the highest ( $p < 0.0001$ ).

The relative gas diffusivity ( $D_s/D_o$ ) at  $-100$  hPa matric potential ranged from  $<0.02$  at the Lithuanian and Dutch sites to  $>0.03$  at the Swedish and Danish sites. The specific gas diffusivity ( $SD$ ) ranged from around  $0.08$  at the French, Lithuanian, and Spanish sites to around  $0.16$  at the Danish, Swiss, and Swedish sites. Darcian air permeability ( $k_a$ ) was significantly lower at the Spanish and Lithuanian sites ( $8.31$  and  $14.3 \mu\text{m}^2$ , respectively) and highest at the Swedish site ( $202.0 \mu\text{m}^2$ ). The ratio of apparent to Darcian air permeability (ratio  $R$ ) showed a nearly inverted order of sites, with the lowest ratio  $R$  at the Swedish and Swiss sites ( $0.38$  and  $0.41$ , respectively) and the highest at the Lithuanian ( $0.67$ ) and Spanish ( $0.78$ ) sites. The average effective pore diameter ranged from  $189$  to  $230 \mu\text{m}$  at the Spanish and Lithuanian sites to  $506$  to  $521 \mu\text{m}$  at the Swiss and Swedish sites, respectively.

### 3.2 | Tillage Practice Impact on Topsoil Bulk Properties

Tillage practice significantly affected the degree of compactness and total pore volume ( $\theta$ ) across soil depths and experimental sites (Table 3). The degree of compactness was higher in the no-till than in the ploughed treatments ( $p = 0.003$ ), while total pore volume was highest in the ploughed treatments ( $p = 0.008$ ) (Figure 1). The interaction of tillage practice and soil depth significantly affected  $\epsilon_a$  and  $WFSP$  at each matric potential (Table 3). The  $\epsilon_a$  was highest and  $WFPS$  lowest in the ploughed  $0$ – $0.10$  m soil layer ( $p < 0.001$ ), with no significant differences between the other combinations of tillage practice and soil depth (Figure 1).

Differences in the bulk properties between the two soil layers, across tillage practices, varied between sites (Table 3, see also Figure S3). At the Swedish site, the degree of compactness and  $WFPS$  were lower (Figure 2) whilst the total pore volume was higher in the  $0$ – $0.10$  m than in the  $0.10$ – $0.20$  m soil layer ( $p < 0.001$ ). At the French site, the degree of compactness and total pore volume showed the same differences (both  $p < 0.003$ ), but  $WFPS$  did not differ between soil layers (Figure 2, with  $p = 0.059$  for  $WFPS_{-100}$ ). The total pore volume was also largest in the  $0$ – $0.10$  m soil layer at the Danish ( $p = 0.016$ ) and Lithuanian ( $p = 0.004$ ) sites. For the latter,  $WFPS_{-60}$  and  $WFPS_{-100}$  were lowest in the  $0$ – $0.10$  m soil layer ( $p = 0.020$  and  $0.009$ , respectively).

### 3.3 | Tillage Practice Impacts on Topsoil Gas Transport Characteristics

The interaction of tillage practice and soil depth significantly affected  $D_s/D_o$  across locations ( $p = 0.035$ ) (Table 3). The  $D_s/D_o$  was highest in the ploughed  $0$ – $0.10$  m soil layer ( $p \leq 0.009$ )

(Figure 3). No significant differences were found between the other combinations of tillage and depth, although  $D_s/D_o$  was noticeably higher in the no-till  $0$ – $0.10$  m than in the no-till  $0.10$ – $0.20$  m soil layer ( $p = 0.056$ ). Despite the overall effect,  $D_s/D_o$  varied between tillage and depth at some sites as indicated by the interaction effects (Table 3, Figure 4 top). The  $D_s/D_o$  was higher in the ploughed than in the no-till treatment at the Danish ( $p = 0.003$ ) and French ( $p = 0.031$ ) sites and was higher in the  $0$ – $0.10$  m than in the  $0.10$ – $0.20$  m soil layer at the Swedish ( $p < 0.001$ ) and French ( $p < 0.001$ ) sites (see also Figure S3).

The specific diffusivity was higher in the  $0$ – $0.10$  m than in the  $0.10$ – $0.20$  m soil layer ( $p < 0.001$ ) with no difference between tillage practices (Table 3, Figure 3). The  $k_a$  was higher in the ploughed than in the no-till treatment at the Lithuanian site ( $p < 0.001$ ), and near-significant differences were found at the Swedish and French sites (Figure 4, bottom). The  $k_a$  was higher in the  $0$ – $0.10$  m than in the  $0.10$ – $0.20$  m soil layer at the Swedish, Dutch, and French sites, while the opposite was found at the Spanish site. The ratio  $R$  was higher in the no-till than in the ploughed treatment at the Lithuanian ( $p < 0.001$ ) and French ( $p = 0.038$ ) sites, higher in the  $0.10$ – $0.20$  m than in the  $0$ – $0.10$  m soil layer at the Dutch ( $p = 0.021$ ) and French ( $p = 0.112$ ) sites, and higher in the  $0$ – $0.10$  m than in the  $0.10$ – $0.20$  m soil layer at the Spanish site ( $p = 0.045$ ) (see also Figure S3).

The effect of the interaction of tillage practice and soil depth on average effective pore diameter varied between sites ( $p = 0.045$ ) (Table 3). The post hoc analyses revealed a larger average effective pore diameter in the no-till  $0$ – $0.10$  m soil layer than in the ploughed  $0$ – $0.10$  m soil layer at the Swedish site ( $634$  and  $397 \mu\text{m}$ , respectively,  $p = 0.016$ ). No differences in average effective pore diameter were found between any of the combinations of tillage and depth at the other sites ( $p \geq 0.065$ ). The significant interaction between tillage and site across soil depths was evidenced by the larger average effective pore diameter in the ploughed ( $294 \mu\text{m}$ ) than in the no-till treatment ( $165 \mu\text{m}$ ) at the Lithuanian site ( $p = 0.022$ ), in addition to an effect at the Swedish site (Table 3).

### 3.4 | Modelling Gas Transport Characteristics Across the Pedoclimatic Gradient

The fitting of  $D_s/D_o$  and the volume of air-filled pores with an equivalent diameter  $\geq 30 \mu\text{m}$  ( $\epsilon_{a-\theta \geq 30 \mu\text{m}}$ ) using the macroporosity-dependent (MPD) model by Moldrup et al. (2000) resulted in a significantly different model for the  $0$ – $0.10$  m than the  $0.10$ – $0.20$  m soil layer ( $p = 0.032$ ) and indicated a stronger increase in  $D_s/D_o$  with  $\epsilon_{a-\theta \geq 30 \mu\text{m}}$  in the  $0$ – $0.10$  m than in the  $0.10$ – $0.20$  m soil layer (Table 4). However, the relationship between  $D_s/D_o$  and  $\epsilon_{a-\theta \geq 30 \mu\text{m}}$  was better described in the  $0$ – $0.10$  m soil layer than in the  $0.10$ – $0.20$  m soil layer ( $R^2 = 0.70$  and  $0.44$ , respectively), and the difference in AIC values of these depth-specific MPD models was substantial, with the MPD model based on all being the best performing (Table 4). With the MPD model,  $\epsilon_a$  explained 59% of the variance of  $D_s/D_o$  across tillage practice, depths, and site. The water-induced linear reduction (WLR) model by Marshall (1959) performed poorest, with an

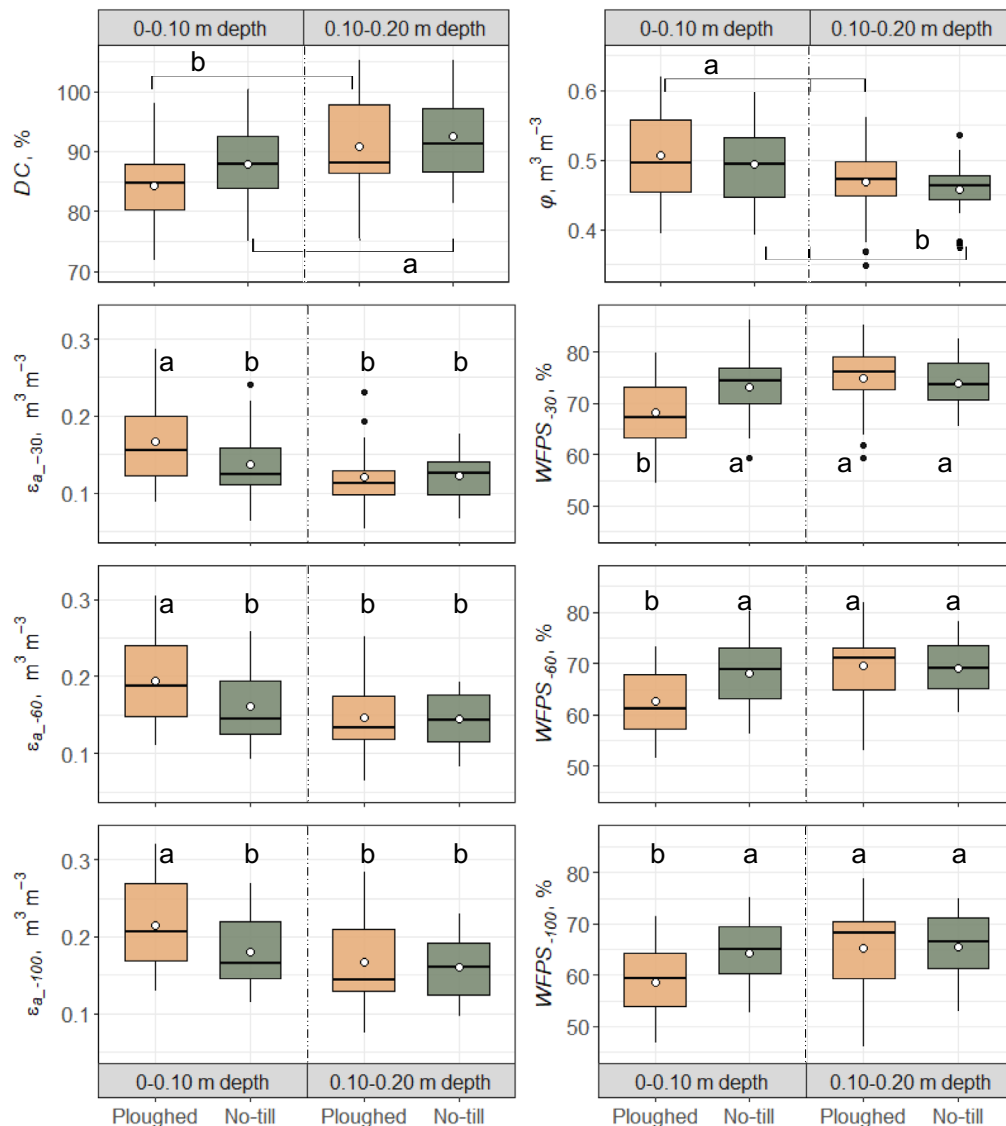


**FIGURE 1** | Soil bulk properties across sites ( $N=28$  per treatment  $\times$  depth). Boxplots display the median (central line), interquartile range (IQR, box), and whiskers (indicating data points within 1.5 times the IQR). White points represent the estimated means and the black points outside the whiskers represent potential outliers.  $DC$ =degree of compactness;  $\phi$ =total pore volume;  $\epsilon_a$ =air-filled pore volume at  $-30$ ,  $-60$ , and  $-100$  hPa matric potential;  $WFPS$ =water-filled pore space at  $-30$ ,  $-60$ , and  $-100$  hPa matric potential. Different letters indicate significant differences between tillage treatments ( $DC$  and  $\phi$ ) or between the interaction of tillage practices and soil depth or at the 0.05 significance level (see Table 3 for analysis of variance). The data per location (mean and standard deviation,  $N=4$ ) are visualised in Figure S3.

AIC difference of 569 and  $R^2$  of 0.48. The simplest model included, based on Buckingham (1904), performed second-best with an AIC difference of 29. This model predicted a lower  $D_s/D_o$  for a given  $\epsilon_{a-\theta \geq 30 \mu m}$  than the MPD model up to an  $\epsilon_{a-\theta \geq 30 \mu m}$  value of around  $0.22 \text{ m}^3 \text{ m}^{-3}$  and a higher  $D_s/D_o$  beyond this level (Figure 5). Despite an acceptable overall model fit, the models overpredicted  $D_s/D_o$  at the French site and underpredicted  $D_s/D_o$  at the Swiss and Swedish sites in both tillage treatments (Figure 5).

The  $k_a$ , measured at  $-100$  hPa matric potential, was better described by  $\epsilon_a$  at  $-30$  hPa ( $\epsilon_{a-\theta \geq 100 \mu m}$ ) than at  $-100$  hPa matric potential ( $R^2=0.30$  and  $0.14$ , and  $AIC=172$  and  $197$ , respectively) (Figure 6,  $p<0.001$ ). While  $\epsilon_{a-\theta \geq 100 \mu m}$  explained more of the variation of  $k_a$  in the  $0-0.10 \text{ m}$  than in the  $0.10-0.20 \text{ m}$

soil layer, no significant differences in coefficients were found between the two soil layers ( $p=0.763$ ).

## 4 | Discussion

### 4.1 | Tillage-Induced Differences in Topsoil Structure Across a Pedoclimatic Gradient

The relative gas diffusivity ( $D_s/D_o$ ) and specific diffusivity ( $SD$ ) indicated differences in the pore functionality between the mouldboard ploughed and no-till soils. The absence of a significant tillage effect on  $SD$  in combination with the interaction effect of tillage and depth on  $D_s/D_o$  (Table 3) indicates that the tortuosity of the vertical pores was greater or that the

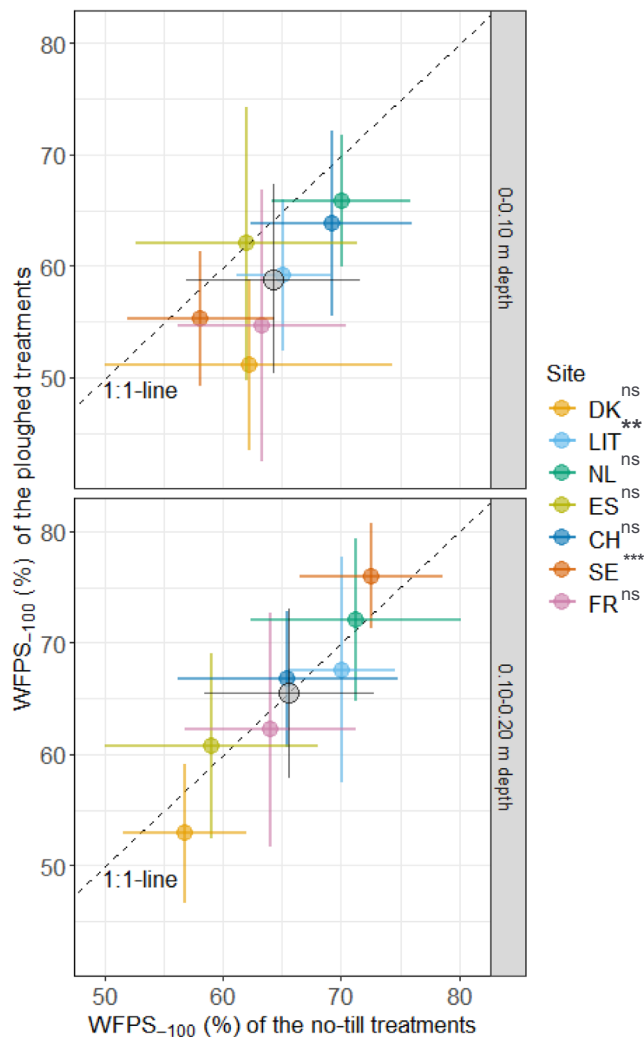


**FIGURE 2** | Water-filled pore space at  $-100$  hPa matrix potential ( $WFPS_{-100}$ ) at different locations and soil depths for ploughed and no-till treatments (mean and standard deviation,  $n=4$ ). ● = mean across the locations ( $p=0.004$  for the interaction of treatment and depth). Significant differences between soil depths for a given location are indicated in the legend with: \*\*\*  $\leq 0.001$ ; \*\*  $\leq 0.01$ ; ns  $\geq 0.05$ .

volume of marginal pores that interact with the diffusion process was smaller in the 0–0.10 m soil layer in the no-till than in the ploughed treatments (Schjønning et al. 2013b).

The ploughed soils exhibited clear vertical stratification of the soil physical characteristics within the top 0.2 m, with a more aerated 0–0.10 m than 0.10–0.20 m soil layer (Table 3, Figures 1 and 3). Vertical stratification of soil structural characteristics in ploughed soils has been reported considering topsoil and subsoil (Martínez et al. 2016; Schlüter et al. 2018), yet the results of this study imply that the stratification also occurs within the topsoil where it may affect the functionality of a soil, that is, promote soil processes different from a non-stratified topsoil. This is indicated, for example, by the  $D_s/D_o$ , above and below the common thresholds for oxic soil conditions and aerobic microbial activity of 0.005–0.02 for the ploughed 0–0.10 m and 0.10–0.20 m soil layers (Schjønning et al. 2003; Stepniewski 1981), respectively (Figure 3).

The vertical stratification within the ploughed soils is an expected result of soil structural development including slumping or settlement following ploughing that was greater in the 0.10–0.20 m than in the 0–0.10 m soil layer. During soil settlement, the bulk density increases and the pore size distribution shifts from larger to smaller pores, and differences in characteristics of topsoils under ploughed and no-till practices diminish over time (Geris et al. 2021; Kreiselmeier et al. 2019; Talukder et al. 2022), which are also the case in this study. The soil settlement in the 0.10–0.20 m layer may be greater due to compaction from the mass of the 0–0.10 m soil layer. Moreover, the 0.10–0.20 m soil layer is less exposed to changes in temperature and moisture that stimulate swell-shrink dynamics in soils with active clays than in the 0–0.10 m layer. Considering that long-term no-till soils are relatively stable throughout the seasons (Geris et al. 2021; Schwen et al. 2011; Wardak et al. 2022), greater differences in the soil characteristics between the two tillage practices are to be expected earlier in the season, closer to mouldboard ploughing.

Despite the natural consolidation and the field management-induced consolidation during the growing season, part of the aeration associated with the ploughing persisted after the growing season. These results support the observations from individual long-term tillage experiments where greater topsoil porosity, air permeability, and/or gas diffusivity were reported under ploughed than under no-till practices for at least 6 months after tillage (Abdollahi and Munkholm 2017; Martínez et al. 2016; Schlüter et al. 2018; Talukder et al. 2022).

## 4.2 | Variation Between Sites and Consequences for Model Estimations

Differences in soil structural characteristics between sites, that is, a significant site effect (Table 3), were expected. The effect of site was generally larger than the effects of tillage practice and sampling depth (Figure S3). The site effects may be related to the impact of soil texture and soil organic matter content on soil structure formation and stabilisation (Bronick and Lal 2005). For example, the Danish site's coarse texture has a much higher relative gas diffusivity than the sites with a higher clay content, such as the Dutch, Spanish, and French sites (Figure 4). However, soil texture and soil organic matter content alone do not explain all the site effects observed in this study; the degree of compactness differed significantly between sites despite being normalised for the clay and soil organic matter content. Moreover, the absolute highest and lowest  $D_s/D_o$  values were found for the two sandiest sites (i.e., the Danish and the Lithuanian sites). These results highlight the effect of other factors such as soil compaction, crop rotation, clay mineralogy, chemical composition of the soil organic matter, climate, and biological activity on soil structure (Bronick and Lal 2005; Bryk et al. 2017; Six et al. 2004a).

Some locations were not consistent with the general observed effect of tillage practice as indicated by the interaction effects of site with tillage treatment and with sampling depth (Table 3). Thus, there are both significant and generalisable impacts of tillage practices but also local deviations. This was also shown by the models describing the soil gas transport capacity if we consider that  $D_s/D_o$  and Darcian air permeability ( $k_a$ ) generally increased

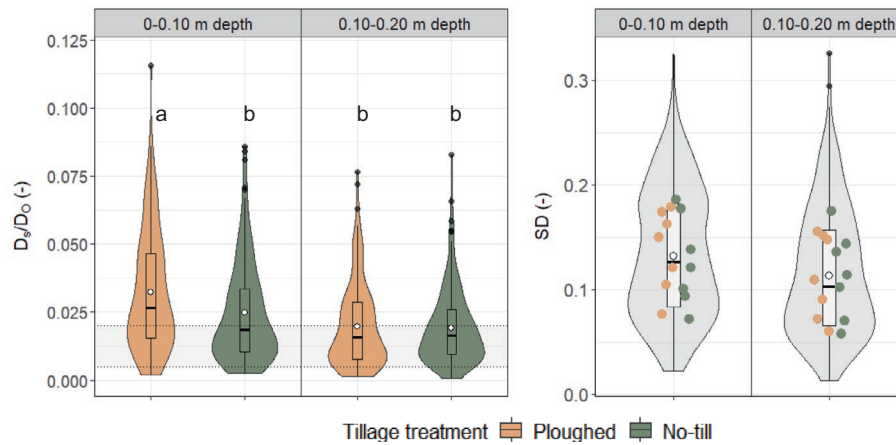


**FIGURE 3** | Relative gas diffusivity ( $D_s/D_o$ , left) and specific gas diffusivity ( $SD$ , right) at  $-100$  hPa matric potential by soil depth and tillage practice, across locations. The violin plot shows the distribution of  $D_s/D_o$ , with the width reflecting the frequency of data points at different values. The boxplot within each violin displays the median (central line), interquartile range (IQR, box), and whiskers (indicating data points within 1.5 times the IQR). Black points outside the whiskers represent potential outliers. ● = estimated mean; The marked area at  $D_s/D_o = 0.005-0.020$  reflects the critical range for oxic soil conditions (e.g., Schjønning et al. (2003)). Different letters indicate significant differences at the 0.95 significance level.

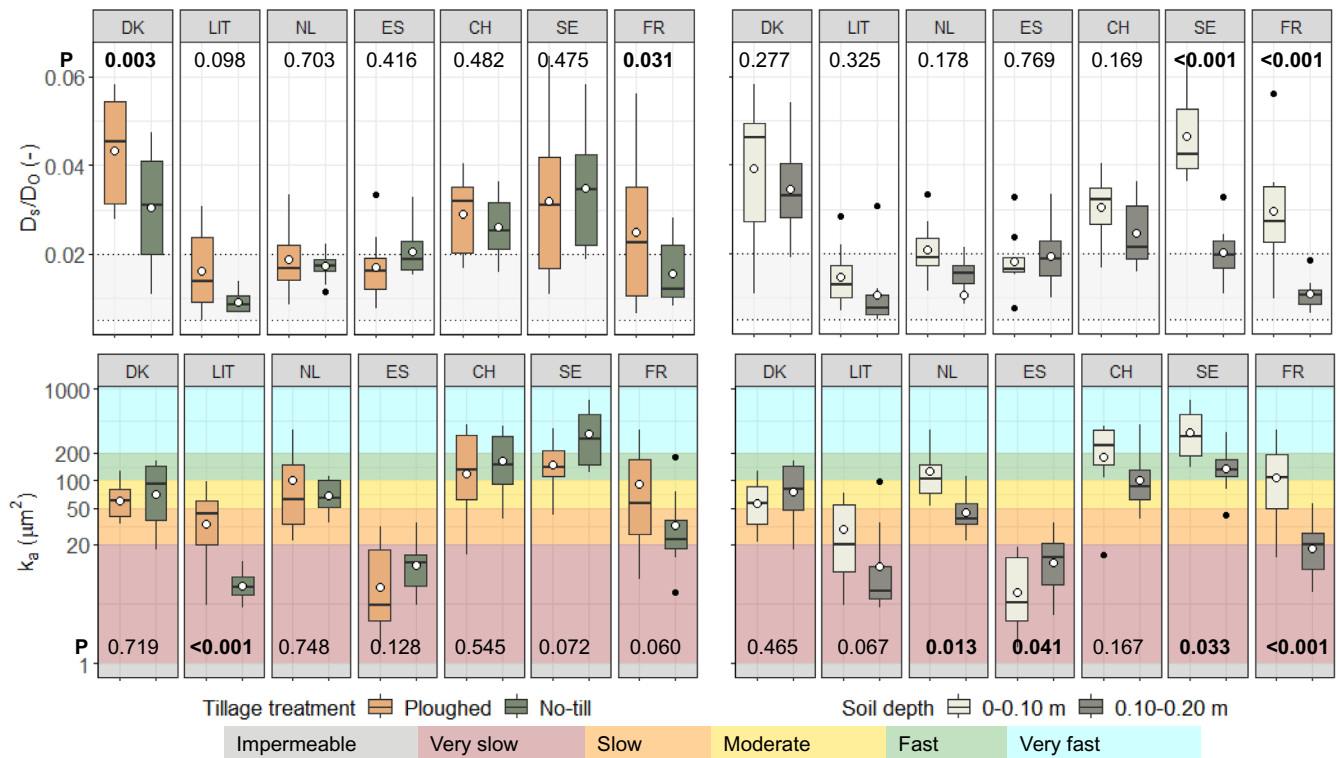


**FIGURE 4** | Top: Relative gas diffusivity ( $D_s/D_o$ ) at  $-100$  hPa matric potential by location and tillage practice (left) and soil depth (right). The marked area at  $D_s/D_o = 0.005-0.020$  reflects the critical range for oxic soil conditions (e.g., Schjønning et al. (2003)). Bottom: Darcian air permeability ( $k_a$ ) at  $-100$  hPa matric potential by location and tillage practice (left) and soil depth (right). The coloured background indicates the classification of air permeability following Fish and Koppi (1994) and Ball et al. (1988). The boxplots display the median (central line), interquartile range (IQR, box), and whiskers (indicating data points within 1.5 times the IQR). Black points outside the whiskers represent potential outliers. ● = estimated mean;  $p$ -values are given per site.

with  $\epsilon_a$  (Buckingham 1904; Moldrup et al. 2000), while sites with greater  $\epsilon_a$  values did not necessarily have higher  $D_s/D_o$  and  $k_a$  values (Figures 5 and 6).

The best-performing models did not differentiate between tillage practices and soil depths. These models explained more of the

variation of  $D_s/D_o$  and  $k_a$  in the 0–0.10 m than in the 0.10–0.20 m soil layer (Figures 5 and 6). While the models performed comparably well for both tillage practices in the 0–0.10 m soil layer, in the 0.10–0.20 m soil layer, more of the variation of  $D_s/D_o$  was explained in the ploughed than in the no-till treatment. Although these results may seem to contradict the significant

**TABLE 4** | Regression models for the prediction of relative gas diffusivity ( $D_s/D_o$ ) from the air-filled pore volume ( $\epsilon_a$ ) at  $-100$  hPa matric potential.

Model	Tillage		Soil depth			Coefficients			Model performance			
	Ploughed	No-till	0–0.10 m	0.10–0.20 m		a	b	c	R <sup>2</sup>	RMSE	AIC	ΔAIC
Buckingham (1904)	$\frac{D_s}{D_o} = \epsilon_a^b$	X	X	X	X	—	2.30***	—	0.52	0.0093	−726	29
	X		X			—	2.34***	—	0.54	0.0100	−566	189
WLR, Marshall (1959)		X	X	X	X	—	2.23***	—	0.54	0.0080	−535	220
	X	X	X			—	2.74***	—	0.48	0.0097	−186	569
MPD—Moldrup et al. (2000)	$\frac{D_s}{D_o} = 2 \cdot \epsilon_a^3 + 0.04 \cdot \epsilon_a$	X	X	X	X	na	na	na	0.51	0.0094	—	—
Best fit	$\frac{D_s}{D_o} = a \cdot \epsilon_a^b + c \cdot \epsilon_a$	X	X	X	X	—	3.11***	0.10***	0.64	0.0081	−755	0
	X	X	X			0.36*	1.58***	—	0.70	0.0080	−595	160
	X	X		X		0.19	1.26**	—	0.44	0.0078	−518	237

Note: The x in the columns Tillage and Soil depth indicates which subset of data was used to extract the coefficients for a given model when the model coefficients differed significantly ( $p < 0.05$ ) between tillage treatments or soil depths. The models in bold are presented in Figure 5.  
Abbreviations: AIC, Akaike Information Criterion; ΔAIC, AIC-difference with best performing model; na, not estimated; ns =  $p > 0.05$ ; RMSE, root mean square error.  
\*\*\* $p < 0.001$ .  
\*\* $p < 0.01$ .  
\* $p < 0.05$ .

vertical stratification observed in the ploughed treatments, they may simply indicate that other pore characteristics besides  $\epsilon_a$ , such as pore connectivity, pore continuity, and pore orientation, can contribute considerably to  $D_s/D_o$  and  $k_a$  in the 0.10–0.20 m soil layer. These characteristics may also explain the deviations of the measured  $D_s/D_o$  and  $k_a$  from the model predictions mentioned above.

Modelling  $k_a$  accurately is generally challenging because  $k_a$  varies greatly in response to changes in the soil structure. However,  $k_a$  is an important regulator of soil aeration and has been found to be a key driver of the N<sub>2</sub>O diffusion ratio in compacted soils (Pulido-Moncada et al. 2024). Previous studies have found  $k_a$  to be a function of the air-filled macropores rather than total air-filled pore volume due to its dependency on the dimensions of the widest pores (Ball 1981b; Martínez et al. 2016). Our results indicate that  $\epsilon_a$  explained more of the variation of the  $k_a$  measured at  $-100$  hPa matric potential when limited to  $>100 \mu\text{m}$  pores (i.e., the equivalent of the  $\epsilon_a$  at  $-30$  hPa matric potential,  $R^2 = 30\%$ ) than for  $>30 \mu\text{m}$  pores (i.e., the equivalent of  $\epsilon_a$  at  $-100$  hPa matric potential,  $R^2 = 14\%$ ).

Further examination of the soil pore characteristics reveals that the over- and underestimations of  $k_a$  (Figure 6) were for cases (i.e., tillage or depth per site) where  $k_a$  was classified as very slow and very fast, respectively (Figure 4). Moreover, the overestimations were for cases with a high ratio  $R$  and small average effective pore diameter ( $d_{\text{eff}}$ ) (Figure S3). The opposite observations were made for the underestimations, which were characterised by a low ratio  $R$  and large average effective pore diameter (Figure S3). This indicates that model estimations of  $k_a$  might improve by accounting for pore turbulence or effective pore diameter.

### 4.3 | Consequences for Soil Functioning

The bulk characteristics of this study indicate that the top-soil structure under both ploughing and no-till may provide a suitable environment for root growth. Both tillage treatments fulfilled the suggested minimum requirement of 10%–15% air-filled pore volume ( $\epsilon_a$ ) for sufficient aeration from a plant production point of view (e.g., Dexter 1988; Grable and Siemer 1968; Wesseling and van Wijk 1957), as extrapolated from Figure 1 (see also Figure S3). Moreover, the degree of compactness (DC) in the 0–0.10 m layer was generally within the optimal degree of compactness range for different crops (including potato (*Solanum tuberosum* L.), oilseed rape (*Brassica* species) and small-grain cereals) of 82%–87% (Håkansson and Lipiec 2000). In the 0.10–0.20 m soil layer, the average degree of compactness of the ploughed and no-till soils exceeded 90%, indicating restricted root growth conditions. Root growth is an important aspect of soil-C-sequestration, as root-derived C is found to be more stable than C derived from aboveground plant residues (Kätterer et al. 2011; Mattila and Vihanto 2024).

After a precipitation event, water infiltration might be greater in the ploughed than in the no-till soils due to the greater volume of drainable pores in the 0–0.10 m soil layer, as indicated by the larger  $\epsilon_a$  at relatively wet soil conditions (i.e., at  $\geq -100$  hPa matric potential) (Figure 1). By contrast, the reduced  $\epsilon_a$  in the

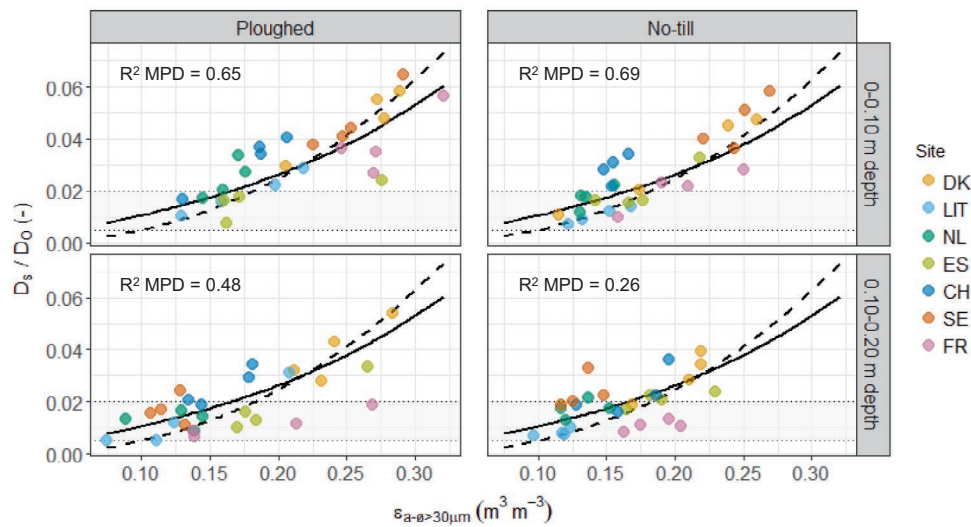


**FIGURE 5** | Relative gas diffusivity ( $D_s/D_0$ ) related to the air-filled pore volume ( $\epsilon_a$ ) at  $-100$  hPa matric potential, that is, when pores  $> 30 \mu\text{m}$  are air-filled ( $\epsilon_{a-\theta > 30 \mu\text{m}}$ ). The marked area at  $D_s/D_0 = 0.005\text{--}0.020$  reflects the critical range for oxic soil conditions (e.g., Schjønning et al. 2003). The solid line shows the fitted macroporosity-dependent model (MPD) by Moldrup et al. (2000):  $D_s/D_0 = b \cdot \epsilon_a^a + c \cdot \epsilon_a$  with  $a = na$ ,  $b = 3.11^{***}$ , and  $c = 0.10^{***}$ , while the dashed line shows the fitted model by Buckingham (1904):  $D_s/D_0 = \epsilon_a^b$  with  $b = 2.30^{***}$  (highlighted in bold in Table 4).

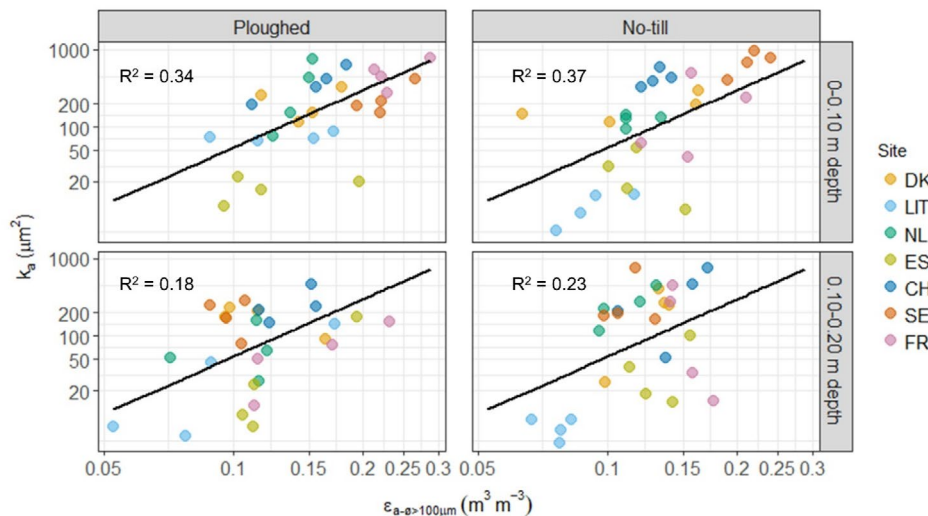


**FIGURE 6** | Darcian air permeability ( $k_a$ ) related to the air-filled pore volume of pores  $> 100 \mu\text{m}$  ( $\epsilon_{a-\theta > 100 \mu\text{m}}$ ), that is, air-filled at  $-30$  hPa matric potential). Solid lines show the fitted linear regression  $\log_{10}(k_a) = M + N \cdot \log_{10}(\epsilon_{a-\theta > 100 \mu\text{m}})$ , with  $M = 4.181$  and  $N = 2.445$ .

ploughed 0.10–0.20 m layer indicates a discontinuity of the pore system within the upper soil layer of the ploughed soil, meaning that water percolation could decrease or cease with soil depth (Logsdon 1995). Poor drainage capacity in wet conditions causes a poor air-water balance, hence soil aeration, and leads to higher denitrification rates. According to a screening by Butterbach-Bahl et al. (2013),  $\text{N}_2\text{O}$  emissions have their optimum in soils with a water-filled pore space (WFPS) of more than 80%. This level was only sporadically exceeded in the soils in this study (Figure S3), with average values at the  $-30$  hPa matric potential ranging from 68.1% to 74.8% for the combinations of tillage and soil depth. However, Pulido-Moncada et al. (2022) conducted a review and found that in compacted soils, WFPS is not a general predictor of  $\text{N}_2\text{O}$  emissions. The authors concluded that the effect of WFPS must interact with other soil properties. Nevertheless, the levels of  $D_s/D_0$  in the 0.10–0.20 m soil layer ( $D_s/D_0 = 0.019$ ,

with a median of 0.016, Figures 3 and 4) indicate that poor aeration may be a problem for coarse-textured soils when considering 0.02 as a critical  $D_s/D_0$  level (Schjønning et al. 2003), even at the  $-100$  hPa matric potential. In the 0–0.10 m layer, aeration was generally good in the ploughed soils ( $D_s/D_0 = 0.032$ , with a median of 0.027) and tended to be more limited in the no-till soils ( $D_s/D_0 = 0.032$ , with a median of 0.019).

Knowing that  $D_s/D_0$  will decrease further at larger soil water contents, it is expected to reach a critically low level earlier during times of wetting under no-till than under ploughed practices. Furthermore, under no-till practices,  $D_s/D_0$  is likely to remain below critically low levels for a longer period during drying, due to the effect of the pore size distributions and geometry on the infiltration, percolation, and retention of water. Such low rates of  $D_s/D_0$  may lead to increased  $\text{N}_2\text{O}$  emissions,

particularly when other soil conditions, such as temperature, pH, nitrate content, and unstable C-availability, are favourable (O'Neill et al. 2020; Rochette 2008). Low  $D_s/D_o$  values may also stimulate complete denitrification, which results in the reduction of  $N_2O$  to  $N_2$  (Balaine et al. 2016), but this depends on pore connectivity, soil depths, and time and distance of gas transport as well as on the microbial community present.

## 5 | Conclusion

The results of this study showed that differences in the soil structural characteristics and their importance for the functionality of long-term ploughed and no-till soils were detectable across a pedoclimatic gradient (sandy loam, loam, silty loam, and silty clay soils). Yet, despite the significant and generalisable impacts of tillage practices, we also observed local deviations. The 0–0.10 m ploughed soil layer displayed the largest air-filled porosity, greatest relative gas diffusivity, and least water-filled pore space, implying the lowest risk of anaerobic soil processes. The 0.10–0.20 m layers of both tillage treatments displayed properties similar to the 0–0.10 m layer in the no-till soils. Larger differences may be expected earlier in the season. Thus, our results indicate that there is a greater risk of poor soil aeration in the upper 0.20 m soil layer under no-till than under ploughing, which increases the risk of  $N_2O$  emissions.

## Author Contributions

**Loraine ten Damme:** data curation, formal analysis, investigation, validation, writing – review and editing, writing – original draft, visualization. **Marta Goberna:** conceptualization, data curation, investigation, funding acquisition, methodology, project administration, validation, supervision, writing – review and editing. **Sara Sánchez-Moreno:** conceptualization, data curation, writing – review and editing, investigation. **Mansonia Pulido-Moncada:** conceptualization, data curation, investigation, methodology, writing – review and editing. **Laurent Philippot:** conceptualization, data curation, writing – review and editing, funding acquisition, investigation. **Mart Ros:** conceptualization, investigation, funding acquisition, writing – review and editing, data curation. **Luca Bragazza:** data curation, investigation, writing – review and editing. **Sara Hallin:** conceptualization, investigation, funding acquisition, writing – review and editing, data curation. **Dalia Feiziene:** conceptualization, investigation, funding acquisition, methodology, writing – review and editing, data curation. **Lars Juhl Munkholm:** conceptualization, investigation, funding acquisition, methodology, data curation, writing – review and editing, supervision, validation.

## Acknowledgements

We thank all the initiators and managers of the seven experimental sites that allowed this study in the first place. Particular acknowledgments go to Cristina Aponte and to all the sampling teams for providing soil samples, to Yves Grosjean (CH), Patricia Plaza, Miguel Ángel Porcel, David San Martín, Javier Sánchez (ES), Arvalis and J. Labreuche (FR), Derk van Balen, Erik Reijnerse, and Kris Huizinga (NL), and Sofia Delin (SE). Special thanks are due to Jørgen M. Nielsen (DK) for the processing of and measurements of the soil samples, and to Maarit Mäenpää (DK) for her rigorous guidance during the statistical analyses.

## Data Availability Statement

The data that support the findings of this study are openly available in Zenodo at <https://zenodo.org/>, <https://doi.org/10.5281/zenodo.13913151>.

## References

- Abdollahi, L., and L. J. Munkholm. 2017. “Eleven Years’ Effect of Conservation Practices for Temperate Sandy Loams: II. Soil Pore Characteristics.” *Soil Science Society of America Journal* 81: 392–403. <https://doi.org/10.2136/sssaj2016.07.0221>.
- Arthur, E., P. Moldrup, P. Schjønning, and L. W. de Jonge. 2012. “Linking Particle and Pore Size Distribution Parameters to Soil Gas Transport Properties.” *Soil Science Society of America Journal* 76: 18–27. <https://doi.org/10.2136/sssaj2011.0125>.
- Badagliacca, G., E. Benítez, G. Amato, et al. 2018. “Long-Term No-Tillage Application Increases Soil Organic Carbon, Nitrous Oxide Emissions and Faba Bean (*Vicia Faba* L.) Yields Under Rain-Fed Mediterranean Conditions.” *Science of the Total Environment* 639: 350–359. <https://doi.org/10.1016/j.scitotenv.2018.05.157>.
- Balaine, N., T. J. Clough, M. H. Beare, S. M. Thomas, and E. D. Meenken. 2016. “Soil Gas Diffusivity Controls  $N_2O$  and  $N_2$  Emissions and Their Ratio.” *Soil Science Society of America Journal* 80: 529–540. <https://doi.org/10.2136/sssaj2015.09.0350>.
- Ball, B. C. 1981a. “Modelling of Soil Pores as Tubes Using Gas Permeabilities, Gas Diffusivities and Water Release.” *Journal of Soil Science* 32: 465–481. <https://doi.org/10.1111/j.1365-2389.1981.tb01723.x>.
- Ball, B. C. 1981b. “Pore Characteristics of Soils From Two Cultivation Experiments as Shown by Gas Diffusivities and Permeabilities and Air-Filled Porosities.” *Journal of Soil Science* 32: 483–498. <https://doi.org/10.1111/j.1365-2389.1981.tb01724.x>.
- Ball, B. C., M. F. O’Sullivan, and R. Hunter. 1988. “Gas Diffusion, Fluid Flow and Derived Pore Continuity Indices in Relation to Vehicle Traffic and Tillage.” *Journal of Soil Science* 39: 327–339.
- Bateman, E. J., and E. M. Baggs. 2005. “Contributions of Nitrification and Denitrification to  $N_2O$  Emissions From Soils at Different Water-Filled Pore Space.” *Biology and Fertility of Soils* 41, no. 6: 379–388. <https://doi.org/10.1007/s00374-005-0858-3>.
- Bates, D., M. Mächler, B. Bolker, and S. Walker. 2015. “Fitting Linear Mixed-Effects Models Using lme4.” *Journal of Statistical Software* 67: 1–48. <https://doi.org/10.18637/jss.v067.i01>.
- Blanco-Canqui, H., and S. J. Ruis. 2018. “No-Tillage and Soil Physical Environment.” *Geoderma* 326: 164–200. <https://doi.org/10.1016/j.geoderma.2018.03.011>.
- Bösch, Y., C. M. Jones, R. Finlay, et al. 2022. “Minimizing Tillage Modifies Fungal Denitrifier Communities, Increases Denitrification Rates and Enhances the Genetic Potential for Fungal, Relative to Bacterial, Denitrification.” *Soil Biology and Biochemistry* 170: 108718. <https://doi.org/10.1016/j.soilbio.2022.108718>.
- Bronick, C. J., and R. Lal. 2005. “Soil Structure and Management: A Review.” *Geoderma* 124: 3–22. <https://doi.org/10.1016/j.geoderma.2004.03.005>.
- Bryk, M., B. Kołodziej, A. Słowińska-Jurkiewicz, and M. Jaroszuk-Sierocińska. 2017. “Evaluation of Soil Structure and Physical Properties Influenced by Weather Conditions During Autumn-Winter-Spring Season.” *Soil and Tillage Research* 170: 66–76. <https://doi.org/10.1016/j.still.2017.03.004>.
- Buckingham, E. 1904. “Contributions to Our Knowledge of the Aeration of Soils (Tech. Rep. 25),” Bureau of Soils, USDA.
- Butterbach-Bahl, K., E. M. Baggs, M. Dannenmann, R. Kiese, and S. Zechmeister-Boltenstern. 2013. “Nitrous Oxide Emissions From Soils: How Well Do We Understand the Processes and Their Controls?” *Philosophical Transactions of the Royal Society B* 368: 20130122. <https://doi.org/10.1098/rstb.2013.0122>.
- Colombi, T., F. Walder, L. Büchi, et al. 2019. “On-Farm Study Reveals Positive Relationship Between Gas Transport Capacity and Organic Carbon Content in Arable Soil.” *Soil* 5: 91–105. <https://doi.org/10.5194/soil-5-91-2019>.

- Cooper, H. V., S. Sjögersten, R. M. Lark, and S. J. Mooney. 2021. "To Till or Not to Till in a Temperate Ecosystem? Implications for Climate Change Mitigation." *Environmental Research Letters* 16, no. 5: 054022. <https://doi.org/10.1088/1748-9326/abe74e>.
- Cosentino, V. R. N., S. A. Figueiro Auregui, and M. A. Taboada. 2013. "Hierarchy of Factors Driving N<sub>2</sub>O Emissions in Non-Tilled Soils Under Different Crops." *European Journal of Soil Science* 64: 550–557. <https://doi.org/10.1111/ejss.12080>.
- ten Damme, L., M. Goberna, S. Sánchez-Moreno, et al. 2024. "TRACE-Soils, LTES Soil Physical Data (Version v1) [Data set]." *Zenodo*. <https://doi.org/10.5281/zenodo.13913150>.
- Dekkers, M. S., M. Trip, D. van Balen, et al. 2023. *Effects of Reduced Tillage on (Cash) Crop Yields, Soil Quality and Other Ecosystem Services: Results From 2009 Till 2022 of the Long Term Experiment BASIS, the Netherlands*. Wageningen University & Research.
- Dexter, A. R. 1988. "Advances in Characterization of Soil Structure." *Soil and Tillage Research* 11: 199–238. [https://doi.org/10.1016/0167-1987\(88\)90002-5](https://doi.org/10.1016/0167-1987(88)90002-5).
- Elberling, B. B., G. M. Kovács, H. F. E. Hansen, et al. 2023. "High Nitrous Oxide Emissions From Temporary Flooded Depressions Within Croplands." *Communications Earth & Environment* 4: 1–9. <https://doi.org/10.1038/s43247-023-01095-8>.
- Fernández-Ortega, J., J. Álvaro-Fuentes, and C. Cantero-Martínez. 2023. "The Use of Double-Cropping in Combination With No-Tillage and Optimized Nitrogen Fertilization Reduces Soil N<sub>2</sub>O Emissions Under Irrigation." *Science of the Total Environment* 857: 159458. <https://doi.org/10.1016/j.scitotenv.2022.159458>.
- Fernández-Ugalde, O., A. Orgiazzi, E. Lugato, and P. Panagos. 2018. "LUCAS 2018: SOIL COMPONENT: Sampling Instructions for Surveyors," EUR 28501 EN.
- Fish, A. N., and A. J. Koppi. 1994. "The Use of a Simple Field Air Permeameter as a Rapid Indicator of Functional Soil Pore Space." *Geoderma* 63: 255–264 0016-7061/94/\$07.00.
- Gee, G. W., and J. W. Bauder. 2018. "Particle-Size Analysis." In *Methods of Soil Analysis. Part 1. Physical and Mineralogical Methods*, edited by A. Klute, 2nd ed., 383–411. Soil Science Society of America, American Society of Agronomy. <https://doi.org/10.2136/sssabookser5.1.2ed.c15>.
- Geris, J., L. Verrot, L. Gao, et al. 2021. "Importance of Short-Term Temporal Variability in Soil Physical Properties for Soil Water Modelling Under Different Tillage Practices." *Soil and Tillage Research* 213: 105132. <https://doi.org/10.1016/j.still.2021.105132>.
- Gómez-Muñoz, B., L. S. Jensen, L. J. Munkholm, J. E. Olesen, E. Möller Hansen, and S. Bruun. 2021. "Long-Term Effect of Tillage and Straw Retention in Conservation Agriculture Systems on Soil Carbon Storage." *Soil Science Society of America Journal* 85: 1465–1478. <https://doi.org/10.1002/saj2.20312>.
- Grable, A. R., and E. G. Siemer. 1968. "Effects of Bulk Density, Aggregate Size, and Soil Water Suction on Oxygen Diffusion, Redox Potentials, and Elongation of Corn Roots." *Soil Science Society of America Journal* 32: 180–186. <https://doi.org/10.2136/sssaj1968.03615995003200020011x>.
- Gradwell, M. W. 1961. "A Laboratory Study of the Diffusion of Oxygen Through Pasture-Topsoils." *New Zealand Journal of Science* 4: 250–270.
- Håkansson, I. 1990. "A Method for Characterizing the State of Compactness of the Plough Layer." *Soil and Tillage Research* 16: 105–120.
- Håkansson, I., and J. Lipiec. 2000. "A Review of the Usefulness of Relative Bulk Density Values in Studies of Soil Structure and Compaction." *Soil and Tillage Research* 53: 71–85. [https://doi.org/10.1016/S0167-1987\(99\)00095-1](https://doi.org/10.1016/S0167-1987(99)00095-1).
- Hallin, S., L. Philippot, F. E. Löffler, R. A. Sanford, and C. M. Jones. 2018. "Genomics and Ecology of Novel N<sub>2</sub>O-Reducing Microorganisms." *Trends in Microbiology* 26: 43–55. <https://doi.org/10.1016/j.tim.2017.07.003>.
- Harris, E., E. Diaz-Pines, E. Stoll, et al. 2021. "Denitrifying Pathways Dominate Nitrous Oxide Emissions From Managed Grassland During Drought and Rewetting." *Science Advances* 7: eabb7118. <https://doi.org/10.1126/sciadv.abb7118>.
- Hill, R. L. 1990. "Long-Term Conventional and no-Tillage Effects on Selected Soil Physical Properties." *Soil Science Society of America Journal* 54: 161–166. <https://doi.org/10.2136/sssaj1990.03615995005400010025x>.
- Huang, Y., W. Ren, L. Wang, et al. 2018. "Greenhouse Gas Emissions and Crop Yield in No-Tillage Systems: A Meta-Analysis." *Agriculture, Ecosystems and Environment* 268: 144–153. <https://doi.org/10.1016/j.agee.2018.09.002>.
- Kätterer, T., M. A. Bolinder, O. Andrén, H. Kirchmann, and L. Menichetti. 2011. "Roots Contribute More to Refractory Soil Organic Matter Than Above-Ground Crop Residues, as Revealed by a Long-Term Field Experiment." *Agriculture, Ecosystems and Environment* 141: 184–192. <https://doi.org/10.1016/j.agee.2011.02.029>.
- Keller, T., and I. Håkansson. 2010. "Estimation of Reference Bulk Density From Soil Particle Size Distribution and Soil Organic Matter Content." *Geoderma* 154: 398–406. <https://doi.org/10.1016/j.geoderma.2009.11.013>.
- van Kessel, C., R. Venterea, J. Six, M. A. Adviento-Borbe, B. Linquist, and K. J. van Groenigen. 2013. "Climate, Duration, and N Placement Determine N<sub>2</sub>O Emissions in Reduced Tillage Systems: A Meta-Analysis." *Global Change Biology* 19: 33–44. <https://doi.org/10.1111/j.1365-2486.2012.02779.x>.
- Kreiselmeier, J., P. Chandrasekhar, T. Weninger, et al. 2019. "Quantification of Soil Pore Dynamics During a Winter Wheat Cropping Cycle Under Different Tillage Regimes." *Soil and Tillage Research* 192: 222–232. <https://doi.org/10.1016/j.still.2019.05.014>.
- Kuncoro, P. H., K. Koga, N. Satta, and Y. Muto. 2014. "A Study on the Effect of Compaction on Transport Properties of Soil Gas and Water I: Relative Gas Diffusivity, Air Permeability, and Saturated Hydraulic Conductivity." *Soil and Tillage Research* 143: 172–179. <https://doi.org/10.1016/j.still.2014.02.006>.
- Lenth, R. V. 2024. "emmeans: Estimated Marginal Means, aka Least-Squares Means," R Packag. version 1.10.2.
- Logsdon, S. 1995. "Flow Mechanisms Through Continuous and Buried Macropores." *Soil Science* 160: 237–242.
- Lucas, M., L. Rohe, B. Apelt, et al. 2024. "The Distribution of Particulate Organic Matter in the Heterogeneous Soil Matrix - Balancing Between Aerobic Respiration and Denitrification." *Science of the Total Environment* 951: 175383. <https://doi.org/10.1016/j.scitotenv.2024.175383>.
- Lucas, M., J. P. Santiago, J. Chen, A. Guber, and A. Kravchenko. 2023. "The Soil Pore Structure Encountered by Roots Affects Plant-Derived Carbon Inputs and Fate." *New Phytologist* 240: 515–528. <https://doi.org/10.1111/nph.19159>.
- Lucas, M., S. Schlüter, H. J. Vogel, and D. Vetterlein. 2019. "Soil Structure Formation Along an Agricultural Chronosequence." *Geoderma* 350: 61–72. <https://doi.org/10.1016/j.geoderma.2019.04.041>.
- Maenhout, P., C. Di Bene, M. L. Cayuela, et al. 2024. "Trade-Offs and Synergies of Soil Carbon Sequestration: Addressing Knowledge Gaps Related to Soil Management Strategies." *European Journal of Soil Science* 75: 1–21. <https://doi.org/10.1111/ejss.135153>.
- Marshall, T. J. 1959. "The Diffusion of Gases Through Porous Media." *Journal of Soil Science* 10: 79–82.
- Martínez, I., A. Chervet, P. Weisskopf, W. G. Sturny, J. Rek, and T. Keller. 2016. "Two Decades of No-Till in the Oberacker Long-Term Field Experiment: Part II. Soil Porosity and Gas Transport Parameters." *Soil and Tillage Research* 163: 130–140. <https://doi.org/10.1016/j.still.2016.05.020>.

- Mattila, T. J., and N. Vihanto. 2024. "Agricultural Limitations to Soil Carbon Sequestration: Plant Growth, Microbial Activity, and Carbon Stabilization." *Agriculture, Ecosystems and Environment* 367: 108986. <https://doi.org/10.1016/j.agee.2024.108986>.
- Metzger, M. J., R. G. H. Bunce, R. H. G. Jongman, C. A. Múcher, and J. W. Watkins. 2005. "A Climatic Stratification of the Environment of Europe." *Global Ecology and Biogeography* 14: 549–563. <https://doi.org/10.1111/j.1466-822X.2005.00190.x>.
- Meurer, K. H. E., N. R. Haddaway, M. A. Bolinder, and T. Kätterer. 2018. "Tillage Intensity Affects Total SOC Stocks in Boreo-Temperate Regions Only in the Topsoil—A Systematic Review Using an ESM Approach." *Earth-Science Reviews* 177: 613–622. <https://doi.org/10.1016/j.earscirev.2017.12.015>.
- Moldrup, P., T. Olesen, P. Schjønning, T. Yamaguchi, and D. E. Rolston. 2000. "Predicting the Gas Diffusion Coefficient in Undisturbed Soil From Soil Water Characteristics." *Soil Science Society of America Journal* 64: 94–100. <https://doi.org/10.2136/sssaj2000.64194x>.
- Mondal, S., and D. Chakraborty. 2022. "Global Meta-Analysis Suggests That No-Tillage Favourably Changes Soil Structure and Porosity." *Geoderma* 405: 115443. <https://doi.org/10.1016/j.geoderma.2021.115443>.
- O'Neill, M., L. Gallego-Lorenzo, G. J. Lanigan, P. D. Forristal, and B. A. Osborne. 2020. "Assessment of Nitrous Oxide Emission Factors for Arable and Grassland Ecosystems." *Journal of Integrative Environmental Sciences* 17: 165–185. <https://doi.org/10.1080/1943815X.2020.1825227>.
- Or, D., T. Keller, and W. H. Schlesinger. 2021. "Natural and Managed Soil Structure: On the Fragile Scaffolding for Soil Functioning." *Soil and Tillage Research* 208: 104912. <https://doi.org/10.1016/j.still.2020.104912>.
- van Ouwerkerk, C., and F. R. Boone. 1970. "Soil-Physical Aspects of Zero-Tillage Experiments." *Netherlands Journal of Agricultural Science* 18: 247–261.
- Petersen, S. O., P. Schjønning, I. K. Thomsen, and B. T. Christensen. 2008. "Nitrous Oxide Evolution From Structurally Intact Soil as Influenced by Tillage and Soil Water Content." *Soil Biology and Biochemistry* 40: 967–977. <https://doi.org/10.1016/j.soilbio.2007.11.017>.
- Pribyl, D. W. 2010. "A Critical Review of the Conventional SOC to SOM Conversion Factor." *Geoderma* 156: 75–83. <https://doi.org/10.1016/j.geoderma.2010.02.003>.
- Pulido-Moncada, M., S. O. Petersen, T. J. Clough, et al. 2024. "Soil Pore Network Effects on the Fate of Nitrous Oxide as Influenced by Soil Compaction, Depth and Water Potential." *Soil Biology and Biochemistry* 197: 109536. <https://doi.org/10.1016/j.soilbio.2024.109536>.
- Pulido-Moncada, M., S. O. Petersen, and L. J. Munkholm. 2022. "Soil Compaction Raises Nitrous Oxide Emissions in Managed Agroecosystems. A Review." *Agronomy for Sustainable Development* 42: 1–26. <https://doi.org/10.1007/s13593-022-00773-9>.
- Rochette, P. 2008. "No-Till Only Increases N<sub>2</sub>O Emissions in Poorly-Aerated Soils." *Soil and Tillage Research* 101: 97–100. <https://doi.org/10.1016/j.still.2008.07.011>.
- Sánchez-Moreno, S., M. Ros, L. ten Damme, et al. 2024. "TRACE-Soils LTER (Long-Term Ecological Research) metadata. Version 1 [Data set]." *Zenodo*. <https://doi.org/10.5281/zenodo.12515043>.
- Schjønning, P. 2019. "A Note on the Forchheimer Approach for Estimating Soil Air Permeability." *Soil Science Society of America Journal* 83: 1067–1072. <https://doi.org/10.2136/sssaj2018.12.0484>.
- Schjønning, P., M. Eden, P. Moldrup, and L. W. de Jonge. 2013a. "Two-Chamber, Two-Gas and One-Chamber, One-Gas Methods for Measuring the Soil-Gas Diffusion Coefficient: Validation and Inter-Calibration." *Soil Science Society of America Journal* 77: 729–740. <https://doi.org/10.2136/sssaj2012.0379>.
- Schjønning, P., and M. Koppelgaard. 2017. "The Forchheimer Approach for Soil Air Permeability Measurement." *Soil Science Society of America Journal* 81: 1045–1053. <https://doi.org/10.2136/sssaj2017.02.0056>.
- Schjønning, P., M. Lamandé, F. E. Berisso, A. Simojoki, L. Alakukku, and R. R. Andreasen. 2013b. "Gas Diffusion, Non-Darcy Air Permeability, and Computed Tomography Images of a Clay Subsoil Affected by Compaction." *Soil Science Society of America Journal* 77: 1977–1990. <https://doi.org/10.2136/sssaj2013.06.0224>.
- Schjønning, P., R. A. McBride, T. Keller, and P. B. Obour. 2017. "Predicting Soil Particle Density From Clay and Soil Organic Matter Contents." *Geoderma* 286: 83–87. <https://doi.org/10.1016/j.geoderma.2016.10.020>.
- Schjønning, P., I. K. Thomsen, P. Moldrup, and B. T. Christensen. 2003. "Linking Soil Microbial Activity to Water- and Air-Phase Contents and Diffusivities." *Soil Science Society of America Journal* 67: 156–165. <https://doi.org/10.2136/sssaj2003.1560>.
- Schlüter, S., C. Großmann, J. Diel, et al. 2018. "Long-Term Effects of Conventional and Reduced Tillage on Soil Structure, Soil Ecological and Soil Hydraulic Properties." *Geoderma* 332: 10–19. <https://doi.org/10.1016/j.geoderma.2018.07.001>.
- Schwen, A., G. Bodner, and W. Loiskandl. 2011. "Time-Variable Soil Hydraulic Properties in Near-Surface Soil Water Simulations for Different Tillage Methods." *Agricultural Water Management* 99: 42–50. <https://doi.org/10.1016/j.agwat.2011.07.020>.
- Shakoor, A., M. Shahbaz, T. H. Farooq, et al. 2021. "A Global Meta-Analysis of Greenhouse Gases Emission and Crop Yield Under No-Tillage as Compared to Conventional Tillage." *Science of the Total Environment* 750: 142299. <https://doi.org/10.1016/j.scitotenv.2020.142299>.
- Six, J., H. Bossuyt, S. Degryze, and K. Denef. 2004a. "A History of Research on the Link Between (Micro)aggregates, Soil Biota, and Soil Organic Matter Dynamics." *Soil and Tillage Research* 79: 7–31. <https://doi.org/10.1016/j.still.2004.03.008>.
- Six, J., S. M. Ogle, F. J. Breidt, R. T. Conant, A. R. Mosiers, and K. Paustian. 2004. "The Potential to Mitigate Global Warming With No-Tillage Management Is Only Realized When Practised in the Long Term." *Global Change Biology* 10: 155–160. <https://doi.org/10.1111/j.1529-8817.2003.00730.x>.
- Stepniewski, W. 1981. "Oxygen Diffusion and Strength as Related to Soil Compaction. II. Oxygen Diffusion Coefficient." *Polish Journal of Soil Science* 14: 3–13.
- Talukder, R., D. Plaza-Bonilla, C. Cantero-Martínez, O. Wendroth, and J. L. Castel. 2022. "Soil Gas Diffusivity and Pore Continuity Dynamics Under Different Tillage and Crop Sequences in an Irrigated Mediterranean Area." *Soil and Tillage Research* 221: 105409. <https://doi.org/10.1016/j.still.2022.105409>.
- Vogeler, I., J. Rogasik, U. Funder, K. Panten, and E. Schnug. 2009. "Effect of Tillage Systems and P-Fertilization on Soil Physical and Chemical Properties, Crop Yield and Nutrient Uptake." *Soil and Tillage Research* 103: 137–143. <https://doi.org/10.1016/j.still.2008.10.004>.
- Wagner-Riddle, C., K. A. Congreves, D. Abalos, et al. 2017. "Globally Important Nitrous Oxide Emissions From Croplands Induced by Freeze–Thaw Cycles." *Nature Geoscience* 10: 279–283. <https://doi.org/10.1038/ngeo2907>.
- Wardak, D. L. R., F. N. Padia, M. I. de Heer, C. J. Sturrock, and S. J. Mooney. 2022. "Zero Tillage has Important Consequences for Soil Pore Architecture and Hydraulic Transport: A Review." *Geoderma* 422: 115927. <https://doi.org/10.1016/j.geoderma.2022.115927>.
- Wesseling, J., and W. R. van Wijk. 1957. "Soil Physical Conditions in Relation to Drain Depth." *Drainage of Agricultural Lands* 7: 461–504.
- Young, T. 1805. "An Essay on the Cohesion of Fluids." *Philosophical Transactions. Royal Society of London* 95: 65–87.

## Supporting Information

Additional supporting information can be found online in the Supporting Information section.